Joule

CellPress

Perspective

Machine Learning for Perovskites' Reap-Rest-Recovery Cycle

John M. Howard,[1,2] Elizabeth M. Tennyson,[1,2] Bernardo R.A. Neves,[2,3] and Marina S. Leite[1,2,*]

Perovskite photovoltaics are efficient and inexpensive, yet their performance is dynamic. In this Perspective, we examine the effects of H_2O, O_2, bias, temperature, and illumination on device performance and recovery. First, we discuss pivotal experiments that evaluate perovskites' ability to go through a reap-rest-recovery (3R) cycle, and how machine learning (ML) can help identify the optimum values for each operating parameter. Second, we analyze perovskite dynamics and degradation, emphasizing the research challenges surrounding this 3R cycle. We then outline experiments that could identify the impact of environmental factors on recovery for different perovskite compositions. Finally, we propose an ML paradigm for maximizing long-term performance and predicting device performance recovery, including a shared-knowledge repository. By reframing perovskites' optoelectronic transiency within the context of recovery rather than degradation, we highlight a set of research opportunities and the artificial intelligence solutions needed for the commercial adoption of these promising solar cell materials.

Introduction

Hybrid organic-inorganic perovskite (HOIP) photovoltaic (PV) devices are an emerging technology with substantial promise, indicated by a record power conversion efficiency (PCE or η) of 23.3%[1] and an average increase of ~2.4% PCE/year.[1] The general perovskite structure is represented as ABX_3, with a monovalent cation placed at the A site, a divalent metal, most often Pb^{2+}, at the B site, and a halide or halide mixture (I^-, Cl^-, or Br^-) occupying the X site. Regarding composition, the A site is predominantly organic, typically formamidinium $CH_3(NH_2)_2^+$ and/or methylammonium $CH_3NH_3^+$. In the last 2 years, researchers have discovered that the addition of small amounts of Cs, and/or Rb, stabilizes the PV thermal and electronic responses.[2,3] This stability enhancement results in more than an order of magnitude increase in the PCE lifetime.[3–5] Concerning other material options, Pb-free alternatives are also being pursued by incorporating Sn, Ti, or Sb as the B site metal,[6–8] in order to allay toxicological concerns.[9]

Despite the above-mentioned meteoric rise in performance, HOIPs present dynamic electrical[10] and optical[11] responses and, often, critical instabilities under the intrinsic and extrinsic working conditions shown in Figure 1A. The effects of extrinsic parameters (the presence of H_2O and O_2) can be potentially mitigated through suitable encapsulation and fabrication strategies. Conversely, the intrinsic parameters are unavoidable during device operation, and defined here as bias, temperature, and light. Therefore, identifying, understanding, and controlling the influence of each one of these factors (as well as their combined effects) toward the stability of HOIPs from the macro- to the nanoscale will continue to be a major thrust in the research community. For instance, there are 31 possible combinations between the five parameters (for each perovskite chemical composition), without considering the order

Context & Scale

High-performing and low-cost photovoltaics (PV) are critical to the continued adoption of renewable energy sources. While promising, perovskite solar materials show a dynamic optoelectronic response when exposed to H_2O, O_2, bias, temperature, or light that severely impacts their performance, preventing commercialization. We posit a reap-rest-recovery cycle to avoid permanent material degradation and achieve long-term power conversion efficiency through machine learning (ML). First, the influence of each above-mentioned parameter must be investigated individually and in combination, from the nano- to the macroscale. With sufficient data for ML, provided by a shared-knowledge repository, monitoring frameworks for perovskite solar cells will be developed to maximize long-term operation by using predictive methods to determine the ideal pathways to recovery through rest. With these milestones achieved, we expect perovskite PV to reach the 25 years T_{80} lifetime requirement.

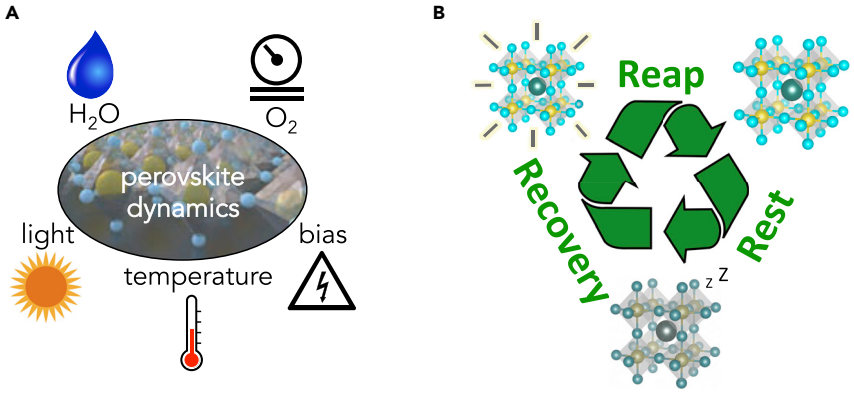

Figure 1. Perovskite Photovoltaic Route to Reliability

(A) Clockwise: extrinsic (H_2O and O_2) and intrinsic (bias, temperature, and light) factors governing dynamics in perovskite solar cells.

(B) The reap-rest-recovery (3R) cycle for obtaining long-term power output from hybrid perovskite solar cells. Operating conditions previously assumed to promote irreversible deterioration need to be reevaluated within the framework of the 3R cycle.

of exposure and the range of values for each. In our opinion, the use of machine learning (ML) is essential to track and predict the influence of each intrinsic and extrinsic parameter on the performance of perovskite solar cells. Thus, the realization of stable perovskite PVs that can deliver reliable power will certainly benefit from the implementation of artificial intelligence (AI) computational methods, as we discuss later.

In this Perspective, we discuss the pressing need for additional research into perovskites to identify and control the reap-rest-recovery (3R) cycle through ML, in both established and emerging material combinations (e.g., Pb-free options) that will lead to reliable PV devices (see Figure 1B). Here, we define recovery in a solar cell device as the ability to restore its PCE after a given amount of time spent under resting conditions, e.g., in the absence of light and bias. A perovskite device initially performs under standard operating conditions, defined here as the reap part of the cycle, where the solar energy is harvested and produces the cell's output power. However, the electrical efficiency of these devices usually deteriorates as a function of time and, therefore, it needs to enter the second phase of the cycle: rest, to avoid permanent material degradation. Given a sufficient rest period under appropriate conditions, the solar cell will have completed the cycle, as it optimally recovers its initial power output. Then, the reap phase begins again. Lastly, we address in detail the powerful role of ML methods for uncovering the ideal 3R operating parameters for HOIP PV over 100 s and eventually 1,000 s of performance cycles. Through this contribution, we provide a framework for an ML approach for obtaining reliable HOIP PV solar cells, which could be expanded to commercial modules.

The Need for Research in HOIP Dynamics and Recovery

Additional research, both fundamental and applied, is required to fully understand and control the dynamics throughout the 3R cycle in state-of-the-art perovskite PV. Degradation in this class of materials has been viewed as a challenge to surmount, with modest attention to the existence and enhancement of performance recovery. HOIP devices of various absorber-layer compositions now have the ability to perform for >1,000 hr,[4–6] without dramatic performance losses (T_{80} > 2,000 hr).[12] Importantly, resting the device without illumination can restore the power output

[1]Department of Materials Science and Engineering, University of Maryland, College Park, MD 20740, USA

[2]Institute for Research in Electronics and Applied Physics, University of Maryland, College Park, MD 20740, USA

[3]Department of Physics, Federal University of Minas Gerais, Belo Horizonte, MG 31270-901, Brazil

*Correspondence: mleite@umd.edu

https://doi.org/10.1016/j.joule.2018.11.010

of some devices to >95% initial values (assuming an inert environment).[13] Regardless of these initial experiments, the amount of work focusing on degradation mechanisms far outweighs the quantity addressing recovery pathways in perovskites of different chemical compositions. Device performance in HOIP is often path dependent with respect to ambient conditions,[11] and degradation studies rarely optimize rest and/or recovery steps. In this section, we outline how micro- and macroscopic methods have been used to tackle perovskite dynamics under distinct environmental factors, emphasizing rest and recovery when appropriate. This discussion is followed by suggestions for future experiments that can provide a robust description of the transient optoelectronic behavior across the entire 3R cycle. Due to the extensive number of perovskites suitable for PV (>9,000),[14] and how each chemical composition has distinct stability limits (i.e., performance response when exposed to the intrinsic and extrinsic parameters displayed in Figure 1A), the implementation of supervised and unsupervised ML routines for the experiments highlighted in this section will enable timely feedback about the conditions for optimizing both rest and recovery.

As expected, an extensive variety of macroscopic measurements addressing the primary factors affecting perovskite dynamics, H_2O, O_2, bias, temperature, and illumination, have been performed.[15,16] In Figure 2, we highlight a subset wherein the 3R cycle has been partially addressed. For example, device efficiency half-life depends substantially on the surrounding ambient, with samples aged in N_2 lasting more than 60× longer than those aged in air containing 100% relative humidity (rH) (see Figure 2A—representing the reap phase). This implies that HOIP solar cells performing in an inert or encapsulated environment can perform longer before needing to rest, as anticipated. Because device performance often decreases as a function of time due to material degradation, the devices must rest for an amount of time that depends on the perovskites' chemical composition, and the environment (including the five parameters displayed in Figure 1A). A rest process for an HOIP solar cell based on a $CH_3NH_3PbI_{3-x}Cl_x$ absorber is shown in Figure 2B. Here, the residual photovoltage in the dark results from the migration of ionic species to the electron transport layer interface, where they act as recombination sites.[17] The rest phase time for this voltage condition strongly depends on the electron transport layer (TiO_2 or Al_2O_3) and injection levels (named low-I_0 and high-I_0). Concerning recovery, this phase heavily depends on the rest conditions. When properly rested, all figures-of-merit of the device can be restored to >70% of their initial values (see Figure 2C for a recovery example).[18] This work shows that the required duration of the rest phase depends on how much performance is lost during the actual solar cell operation. For an HOIP device that decays to 80% (aged to its T_{80} lifetime) of its initial PCE (in blue in the left graph), only 3 hr of rest returns all figures-of-merit to >90% of their starting values. Contrastingly, the same device at 50% of initial power output (see right graph, corresponding to T_{50}) needs more than 30 hr to recover to ~80%.[18] Researchers have also identified HOIP cells with contrary fatigue behavior that recover their performance while under illumination, instead of under dark contitions.[19] Moreover, the restoration behavior can strongly depend on the environmental conditions during aging, where both dark-recovery and light-recovery can occur.[20] These results emphasize the need to comprehensively explore recovery under the five parameters displayed in Figure 1A (both in isolation and when combined) for >100 hr. Because the time and conditions for an effective rest phase strongly depends on the type and the "usage" of the cells, supervised ML is ideal to help deciding the precise values of the extrinsic and intrinsic parameters, as will be discussed in the next section.

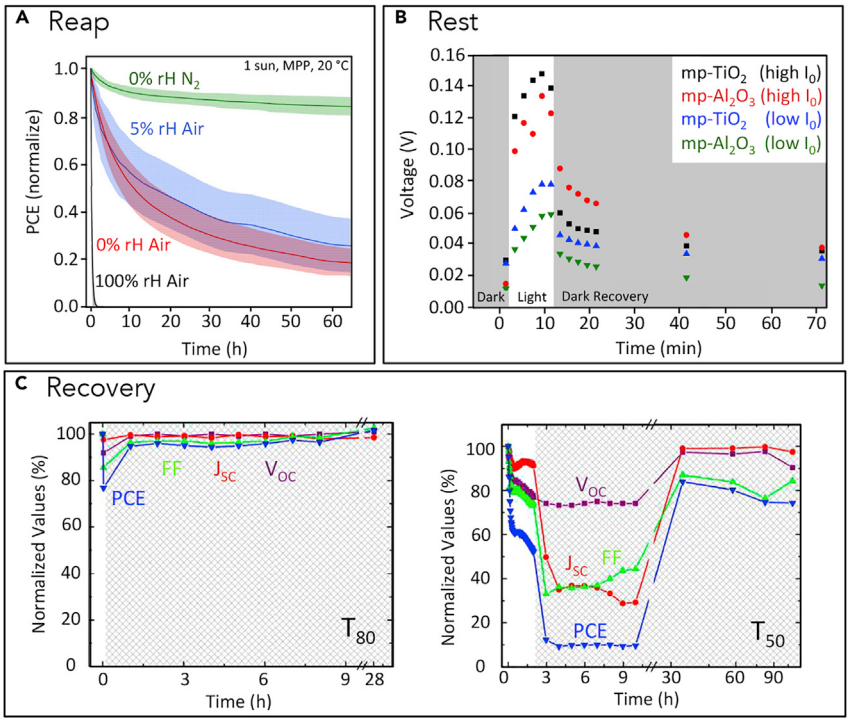

Figure 2. 3R Cycle in Perovskite Solar Cells

(A) In the reap phase, devices provide power. There is an initial exponential decay in performance regardless of ambient gas composition or relative humidity (rH) level. The subsequent performance trend depends on the O_2 and H_2O levels (extrinsic parameters), where devices aged in (1) N_2 (green) shows a clear linear regime, (2) dry air with 5% rH (blue) and with 0% rH (red) continue the decay, and (3) the dry air with 100% rH (black) experiences immediate performance deterioration. In all cases, the shaded area represents the standard deviation. Adapted by permission from Domanski et al.,[12] Springer Nature: Nature Energy, Copyright 2018.

(B) During the rest phase of the cycle, the solar cells are not operational. Here, the rest duration corresponds to the time it takes for the residual voltage under dark conditions to stabilize. Adapted with permission from Hu et al.,[17] copyright 2017 American Chemical Society.

(C) The recovery phase of this cycle takes place when all figures-of-merit return to a substantial fraction of their original values. In this example, greater than 70%, regardless of whether the device was used through its T_{80} or T_{50} lifetime. Adapted with permission from Khenkin et al.,[18] Copyright 2018 American Chemical Society.

To date, the impact of the extrinsic environmental parameters (H_2O and O_2) on the prototypical methylammonium lead triiodide ($MAPbI_3$) composition is relatively well understood compared with other perovskite chemical compositions. Under illumination, O_2 initially passivates this perovskite's defects, but also promotes deterioration of the device's optoelectronic properties.[21] The deleterious effect of O_2, with and without light, is far greater than that of N_2.[22] Macroscopically, the influence of rH has been determined across a range of cation and halide compositions in HOIPs, capturing the rate at which the figures-of-merit diminish.[4,12,23,24] In addition, with *in situ* X-ray diffraction (XRD) analyses, the timescales for emergence of hydrate phases were captured.[25] *In situ* photoluminescence (PL) spectroscopy has also revealed the time-dependence of a perovskite's bandgap on exposure to humidified N_2.[26] Research investigating bias and light (intrinsic parameters) on $MAPbI_3$ found an approximate doubling in both short-circuit current density (J_{sc}) and PCE within 2 min of operation.[27] Long-term measurements have shown that holding triple-cation perovskite devices at V_{oc}, J_{sc}, and maximum power operation point for

<100 hr yields PCE retention of ~55%, >60%, and 75%, respectively.[12] Using temperature as the variable parameter (also an intrinsic factor), researchers have identified the negative effects of temperature extremes (−10°C to 65°C) during 500 hr of logging[12] and the reversibility of $MAPbI_3$ PCE throughout thermal cycles of different bounds.[28] PL spectroscopy has been used extensively to evaluate the dependence of optical stability on both cation and halide composition[29,30] and the influence of wavelength on dynamic photodegradation and photobrightening.[31] In addition, cycling light excitation density under different ambient environments (vacuum, N_2, and air) influences the extent of luminescence recovery, revealing that changes to the PL quantum yield are path and composition dependent.[11,32] In particular, UV light has been shown to cause degradation of perovskite PV output over the course of 1,000 hr. However, these losses can be ~40% recoverable over 10 cycles by alternating between UV and AM1.5G illumination.[33] Note that while we define UV light as an intrinsic parameter, we recognize that it could be considered extrinsic given the option of using UV-blocking encapsulant layers.[12] The substantial variation in performance as a function of illumination conditions urges the realization of supervised and unsupervised ML on perovskite thin films (prior to full device development), where PL measurements are sufficient to determine the conditions for radiative recombination recovery.[11]

Because most perovskites present inhomogeneities at the nano- and microscale, microscopic techniques must be further developed to resolve the relationship between composition, morphology, optical response, and electrical behavior at the intragrain and intergrain length scales.[34–38] Figure 3 displays examples of how microscopic methods have been implemented to help elucidate the dynamic response of this emerging material. Through environmentally controlled micro-PL, the effect of ambient gas and vacuum was identified, showing that the presence of O_2 can lead to an order of magnitude increase in radiative recombination; however, as shown in Figure 3A, not all grains behave identically and the phenomenon is facet dependent.[39] Using wide-field PL imaging, the role of an electric field (bias) on ion migration has been captured in real time.[40] The real-time light-induced dynamics at the nanoscale are accessible through Kelvin-probe force microscopy, identifying intragrain voltage variances of ~300 mV that decay over 128 s after returning to dark conditions (Figure 3B).[10] Photoconductive atomic force microscopy (pc-AFM) has revealed intragrain variations in $MAPbI_3$ device figures-of-merit that can be correlated with surface microstructure.[41] In addition, pc-AFM has been used to image the photoinactive surface regions in temperature-cycled $MAPbI_3$ solar cells.[42] Concerning electron microscopy, temperature-controlled scanning transmission electron microscope holders now allow for mapping halide and Pb migration in a $MAPbI_3$ solar cell.[28] The influence of light has also been resolved at the intergrain level through PL microscopy, shown in Figure 3C, providing evidence of the non-uniform distribution of trap states across a $MAPbI_3$ film.[43] Hyperspectral luminescence imaging has been extended to spatially quantify the quasi-Fermi splitting and identify regions of poor carrier extraction.[44] While $MAPbI_3$ has been used as a "model system" for stability analysis, there is a pressing need to extend these microscopic experiments to other perovskites, including Pb-free options. Thus, we foresee scanning probe and electron microscopies becoming essential characterization tools for *in situ* monitoring of the distinct phases comprising the 3R cycle. The extensive amount of data generated by these microscopic methods requires "big data" analytics[36,45] to correlate the perovskites' structural properties (e.g., grain size and morphology) with the physical quantities that define a high-performance and reliable solar cell. Here, we suggest the creation of a worldwide data repository that would combine information about the types of perovskites and the microscopy

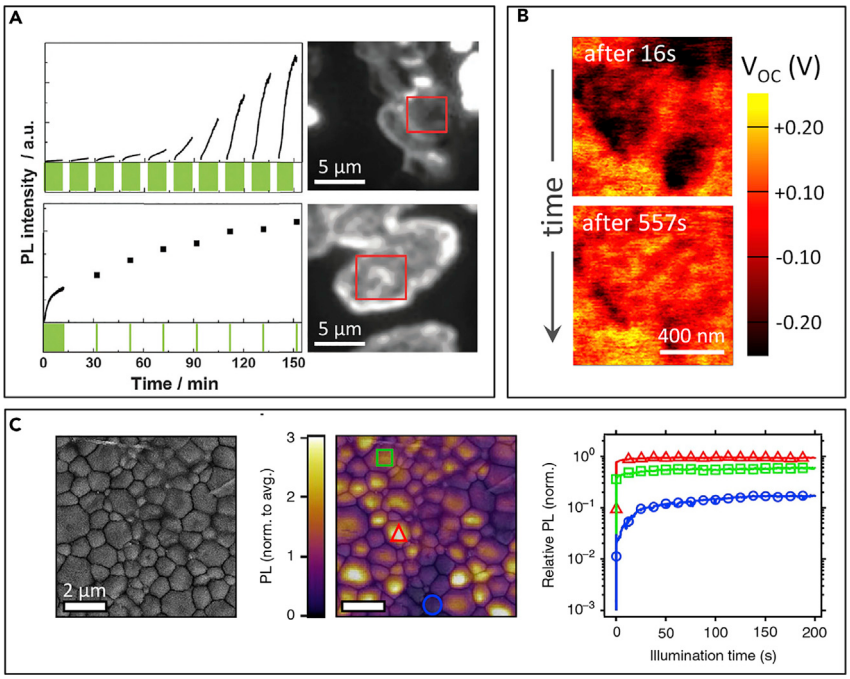

Figure 3. Capturing the Microscopic Optoelectronic Dynamics of Perovskites

(A) The effect of illumination duration (light ON = green and light OFF = white) on the photoluminescence (PL) intensity of different crystal facets. $MAPbI_3$ grains varying in size show radically different dynamics under illumination cycling. Adapted with permission from Tian et al.,[39] published by The Royal Society of Chemistry.

(B) Illuminated-Kelvin-probe force microscopy is used to determine the time-dependent changes in local V_{oc} (1 ms/pixel with 128 × 128 frames). Even within a single grain, the $MAPbI_3$ perovskite exhibits ion motion. Reprinted with permission from Garrett et al.,[10] Copyright 2017 American Chemical Society.

(C) PL imaging establishes the intergrain heterogeneity in $MAPbI_3$ films, and time-dependent measurements reveal the light-emission stabilization. The relative brightness of the grain provides indication of trap state density. Reprinted from deQuilettes et al.,[43] Copyright the authors, some rights reserved; exclusive licensee to Macmillan Publishers Ltd. Distributed under a Creative Commons Attribution Noncommercial License 4.0 (CC BY-NC) http://creativecommons.org/licenses/by-nc/4.0/.

measurement performed, in analogy to the screening of 5,456 oxygen evolution catalysts for artificial photosynthesis.[46] AI routines could perform image analysis in the search for correlation between the datasets acquired by different research groups; see the next section for more details about our proposed approach.

Together, macro- and nanoscale characterization can quantitatively identify the timescale at which rest occurs, as well as how much time is needed for an effective recovery (and the required conditions). Importantly, high-spatial resolution microscopy and diffraction techniques, applied to solar cells throughout their 3R cycle toward recovery, could extract and/or correlate the role of interfaces, grain morphology, size, and composition on the dynamics of device performance. Research into rest will likely shorten the time needed between consecutive reap phases. Given that the bias conditions have an impact on the T_{80} lifetime,[12] it may be possible to use small reverse bias to more quickly return the ionic species to their initial positions. In addition, newer techniques for resolving the local chemical composition, such as photo-induced force microscopy or AFM with infrared spectroscopy, could be applied to device cross-sections at different moments

throughout the 3R cycle to map ion accumulation and depletion at the perovskite-transport layer interfaces. Control of the solar cell's temperature during rest likely impacts the timescales for recovery, and, to date, its effect, static or cycled, remains considerably unexplored. Thus, we propose device cycling with temperature variations during rest (under dark conditions) to determine if the migration rate of ionic species can be controlled. The lowering of temperature while an HOIP device rests without illumination should result in slower recovery as vacancy-mediated ion motion encounters a large activation barrier.[47] Ideally, such temperature cycles would accurately simulate the climate in a number of regions around the world, and thus help predict the behavior of future perovskite PV modules.

ML to Identify and Optimize Device Recovery

ML encompasses the use of algorithms for predictive analysis capable of adapting to the broad scope of the input data. It draws aspects from both computer science and statistics, and has allowed for a number of key advances spanning from humanities to engineering, including speaker recognition,[48,49] autonomous vehicles,[50] traffic predictions,[51] computer vision,[52] protein fold classification,[53] wireless communications,[54] and solar technologies.[55] With the development of user-friendly tools and programming frameworks such as Google's TensorFlow,[56] ML has been applied to an increasingly large set of problems in sustainability that continues to grow in diversity. For instance, engineers have used these techniques to estimate solar module performance under varied cloud conditions, using video streams of the sky as input.[55] AI has been applied toward screening materials for light-absorbing applications, where high-throughput XRD measurements enabled the identification of the phase diagram for a family of Nb-V-Mn oxides from their composition and structural characterization data.[57] Overall, ML has the potential to hasten the energy-related materials development timeline by $\geq$10 times, if infrastructure and human-capital investments are adequately placed.[58]

ML is starting to be implemented in perovskite research, with a modest number of very insightful publications.[14,59] To date, all AI-driven approaches described in the literature focus on the screening of potentially stable chemical compositions. Using a statistical learning model, the evaluation of ~1,300 double perovskite oxides ($AA'BB'O_6$) has shown that their bandgap is largely determined by the lowest occupied energy levels of the A site and by the electronegativities of the B site elements, respectively.[60] The race for non-toxic Pb-free alternatives and the large number of options for the organic and inorganic constituents (>8) has triggered the combination of density functional theory-based high-throughput computational screening with experimental validation.[61] While thus far the effort has been on finding thermodynamically stable perovskites,[59] the community recognizes that this ML method can be expanded to the "characterization" of key physical properties and processes, such as optical response and carrier density. Moreover, ML has been used via unsupervised clustering to resolve the relationship between perovskite structure and the temporal changes in voltage upon light excitation at the nanoscale.[45] These applications highlight the leap enabled by ML in elucidating the perovskites' new chemical compositions and their stability. Yet, tracking the effect of each intrinsic and extrinsic parameter (H_2O, O_2, bias, temperature, and light) on the performance of perovskite solar cells could allow unprecedented control of the conditions for material and device recovery upon rest. Because the influence of each factor on both material stability and device PCE (η) varies if acting alone or when associated with others, it is vital to implement AI routines that can determine the effect of all possible combinations in a timely manner, accelerating knowledge generation for the ultimate commercialization of perovskite PV.

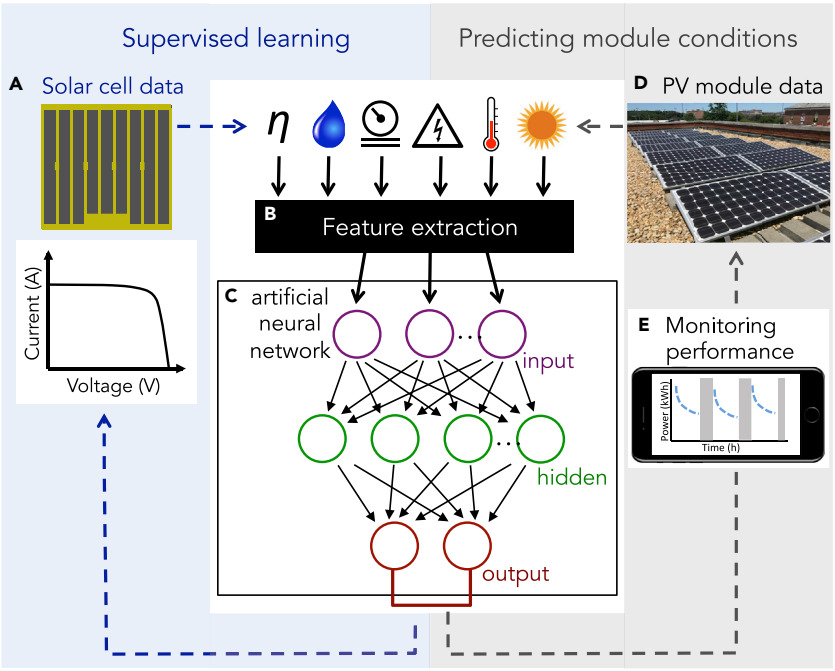

Figure 4. A Machine Learning Framework for a Perovskite 3R Cycle

(A) Time-series laboratory data including the effect of each intrinsic and extrinsic parameter (H_2O, O_2, bias, temperature, and illumination) on device efficiency is used for training the algorithm.

(B) A feature vector is extracted out of the environmental sensor output, together with the solar cell efficiency, η.

(C) An artificial neural network (ANN) is tuned to maximize long-term stability and overall power output.

(D) After the neural network weights are optimized, data from solar modules can be used to determine the rest phase conditions that will lead to recovery and sustained reap.

(E) The future PV module's real-time conditions and performance are displayed onto an internet-connected device, enabling consumers to monitor its 3R cycle.

Our proposed ML framework for optimizing the 3R cycle of perovskite solar cells and future modules considers two parts: one focused on supervised learning of laboratory-scale PV devices, and another where the rest and recovery of modules could be monitored and controlled, as displayed in Figure 4. Initially, the computational framework for the supervised learning steps is optimized using data from thin-film perovskites and laboratory-scale solar cell aging measurements under the five relevant environmental conditions (see Figures 1A and 4A). The training data from devices allow for supervised learning, wherein the model parameters are fitted by comparing its predictions with the known physical outcome as measured using a solar simulator (represented as the left half of Figure 4, in blue). Note that, prior to full device development, an effective characterization of perovskite thin films using ML can identify the relationship between their structural, optical, and electrical properties (including the role of defects and grain boundaries), accelerating the selection of the most promising options to be interrogated as full devices. While the discussion below is focused on full device characterization, we emphasize that the ML methodology proposed could, and should, be expanded to quantifying the effects of the environmental stressors on perovskite materials.

The term "training data," typical to ML applications, refers to data that have known input(s) and output(s) (e.g., PCE). In juxtaposition, "test data" are used to evaluate the smart network software's ability to predict the best operating factors to maximize

performance over the module's lifetime. During preprocessing, the most meaningful attributes (including all environmental stressors: H_2O, O_2, bias, temperature, light, and the solar cell/module efficiency, η) will be extracted using factor analysis methods (Figure 4B), such as principal-component analysis, and constructed into a feature vector containing the most explanatory aspects of the data. The derived values are then used as input to an artificial neural network (ANN),[62] a system of connected nodes with activation functions that change state depending on input (see Figure 4C). Thus, the number of input nodes will match the number of entries in the feature vector. For example, under illumination, O_2 hastens degradation.[21,22] Hence, if its presence would be detected by a gas sensor, (1) the corresponding activation function would change state, and (2) altering the ANN's output to predict the effect on PCE. The ML monitoring framework we outline can be expanded to include active control of the environmental stressors based on device performance. For instance, the applied bias might be lessened or the temperature increased when the algorithm detects the end of the reap phase. The input node for all environmental sensor data can have an activation function that suits the performance dynamics under that condition. While training the ANN with laboratory data, the weights of the various nodes are tuned to maximize performance against a chosen cost function. This metric informs the quality of the prediction by comparing and quantifying the network's output with the known one, i.e., the "real life" values of the training PV devices. After optimization, the ANN is ready to be validated by predicting the performance and operating conditions of an even larger set of solar cells from any laboratory. This step is critical in assessing the algorithm's generality prior to real-world application of our proposed method and informs the need to change the network architecture for better predictions. We suggest the realization of ANNs for this time-series prediction problem given its ability to handle complex non-linear behavior,[51] high-predictive power,[54,55] and the ease of automation.[63]

We envision the adoption of separate ANNs for different perovskite compositions, given the range of performance dynamics for each. For instance, some emerging Pb-free options exhibit efficiencies that increase as a function of time,[6] in contrast to the exponential decay of the reap phase often seen in Cs-mixed HOIPs. Further, we suggest an architecture (i.e., the number of layers and their manner of connectivity) similar to the standard long short-term memory (LSTM) recurrent neural networks,[64] a specific type of ANN, for the outlined approach, given their success in time-series prediction.[50] The use of recurrent ANNs is critical, as the embedded loops within them will provide memory of earlier sections of the PV time-series data. The LSTM algorithm can increase performance further, through the use of a repeating design with four distinct layers. This feature of the network offers improved recall between temporally distant data points. Prior efforts have demonstrated the ability of LSTM networks to make predictions of financial markets,[65] and in our opinion, the cyclic nature of perovskite recovery dynamics fall within the scope of this approach. Recent ML algorithms connecting the Akaike information criterion with sparse identification of non-linear dynamics must also be considered, given their ability to automatically recognize the models that best balance error and overfitting out of a large pool of candidates.[66]

For the second part of our ML framework, we anticipate that, after laboratory-scale validation, a network of solar panels could be tested, and eventually routinely monitored, when deployed in the field (represented by the right half of Figure 4, in gray). These modules (Figure 4D) would be equipped with the necessary detectors to monitor the magnitude of the five parameters. Then, the sensor output would be fed into the previously optimized ML algorithm, where all phases of the 3R cycle

are predicted according to the ANN's calculation. We foresee consumers monitoring the performance of the PV modules, as well as the reap, rest, and recovery stages independently, from any internet-connected device, as suggested in Figure 4E. The assessment of the financial viability of the proposed ML approach for PV modules is outside the scope of this Perspective as we choose to emphasize the proficiency of AI to tackle the 3R cycle of perovskites, instead of the costs associated with it. Nevertheless, transitioning ML from the academic world to the real word must be accompanied by a careful cost analysis of human-capital investments.[58]

Recent aging measurements on perovskite PV indicate that the instrumentation already exists to develop the necessary training datasets across a wide volume of the parameter space, including the subset required by the relevant IEC 61215 solar cell standard.[67] These lab-sourced data are well suited for the development of our ML paradigm as it can inform the system about a PV module's ideal conditions for resting toward its recovery. While some environmental thresholds for rapid performance deterioration have already been established (e.g., 90% rH leading to loss of all PCE in less than 3 hr[12]), still others require additional evaluation. Capturing the influence of all intrinsic parameters on the 3R cycle for the supervised learning stage is critical to the success of the ML approach. Temperature plays a critical role and researchers must perform dark/light cycles with thermal conditions varied to mimic the real-world environments of different regions. For example, the desert areas during the day (~40°C) potentially have shorter reap phases, while their cold nights (~0°C) lengthen recovery. In equatorial regions, the coupling between temperature and humidity is of special interest. Earlier experiments on $MAPbI_3$ found that 24 hr of combined exposure to 85°C and 60% rH led to 4-fold reduction in PCE,[42] stressing the need for (1) robust encapsulation, (2) humidity and temperature tolerant materials and device architectures, and (3) a complete understanding of how this combined effect influences the 3R cycle. Similar experiments need to be replicated on a wide variety of modern perovskite compositions that remain stable both optically and structurally above 85°C.[3] We also note that intermittent or spatially non-uniform illumination of PV modules regularly occurs during operation, but remains predominantly uninvestigated in perovskite solar cell laboratory tests. Heterogeneous illumination presents a serious issue, as shaded regions of a single solar cell experience reverse bias, in contrast to other areas in the device that are under illumination.[68,69] Concerning light treatments, the substantial variety of possible illumination conditions must be emulated at the laboratory scale first in order for the ML analysis to perform well in real-world situations.

The challenges of applying ML to experimental materials science include: (1) collecting sufficient information for the input, (2) aggregating the large amount of data produced from different laboratories, and (3) ensuring that the experimental results are comparable. Here, we suggest that data from laboratories around the world be anonymized and aggregated into a repository database that will eventually lead to supervised knowledge extraction concerning the 3R cycle. Specifically, researchers would share the parameters used for synthesizing the perovskites and the conditions for both the perovskite material (from the macro- to the nanoscale, e.g., XRD and PL microscopy) and full device characterization (e.g., light IV under AM1.5 global illumination)—all valuable input information. Inspired by a recent work on the relevance of failed experiments for ML,[70] we advocate that the success of this shared-knowledge tactic lies in researchers reporting both "positive" and "negative" results: the information concerning high-performance devices and non-working ones is equally important for ML trained on performance data to

predict the 3R cycle conditions as function of perovskite composition. We anticipate that as long as the synthesis and characterization are carefully annotated, the input data will provide rich enough information to validate ML, enabling supervised learning to generate valuable knowledge of perovskite PV.

Summary

State-of-the-art perovskite PV materials often exhibit dynamics, decaying in performance over time. With our proposed 3R cycle combined with an ML paradigm, researchers can begin to take advantage of this HOIP solar cell cyclability feature. Macro- to nanoscale characterization can complement one another to correlate structural, electrical, optical, and chemical properties throughout the perovskite 3R cycle. More importantly, these tools will allow the scientific community to identify the most influential environmental parameters, as well as the cutoff between recovery and degradation. Using this information, advanced computational frameworks based on ML could be quickly developed that maximize overall long-term power output, minimizing material degradation. We foresee AI strategies facilitating rapid knowledge transfer between perovskite laboratory-scale behavior throughout the 3R cycle and PV modules, ultimately enabling reliable perovskite solar cells.

ACKNOWLEDGMENTS

M.S.L. thanks the funding support from the National Science Foundation (ECCS, award 16-10833), and the Ovshinsky Sustainable Energy Fellowship from the American Physical Society. B.R.A.N. thanks the financial support from CAPES-Brazil. J.M.H. and M.S.L. acknowledge the 2018–2019 Harry K. Wells Graduate Fellowship from UMD. E.M.T. and M.S.L. thank the 2017–2018 UMD All-S.T.A.R. Fellowship and the 2017–2018 Hulka Energy Research Fellowship from UMD. The authors thank E. Lee for PV module photograph.

REFERENCES

1. Kojima, A., Teshima, K., Shirai, Y., and Miyasaka, T. (2009). Organometal halide perovskites as visible-light sensitizers for photovoltaic cells. J. Am. Chem. Soc. *131*, 6050–6051.

2. Wu, Y.L., Yan, D., Peng, J., Duong, T., Wan, Y.M., Phang, S.P., Shen, H.P., Wu, N.D., Barugkin, C., Fu, X., et al. (2017). Monolithic perovskite/silicon-homojunction tandem solar cell with over 22% efficiency. Energy Environ. Sci. *10*, 2472–2479.

3. Saliba, M., Matsui, T., Seo, J.Y., Domanski, K., Correa-Baena, J.P., Nazeeruddin, M.K., Zakeeruddin, S.M., Tress, W., Abate, A., Hagfeldt, A., et al. (2016). Cesium-containing triple cation perovskite solar cells: improved stability, reproducibility and high efficiency. Energy Environ. Sci. *9*, 1989–1997.

4. Christians, J.A., Schulz, P., Tinkham, J.S., Schloemer, T.H., Harvey, S.P., de Villers, B.J.T., Sellinger, A., Berry, J.J., and Luther, J.M. (2018). Tailored interfaces of unencapsulated perovskite solar cells for > 1,000 hour operational stability. Nat. Energy *3*, 68–74.

5. Tsai, H., Asadpour, R., Blancon, J.C., Stoumpos, C.C., Durand, O., Strzalka, J.W., Chen, B., Verduzco, R., Ajayan, P.M., Tretiak, S., et al. (2018). Light-induced lattice expansion leads to high-efficiency perovskite solar cells. Science *360*, 67–70.

6. Jokar, E., Chien, C.-H., Fathi, A., Rameez, M., Chang, Y.-H., and Diau, E.W.-G. (2018). Slow surface passivation and crystal relaxation with additives to improve device performance and durability for tin-based perovskite solar cells. Energy Environ. Sci. *11*, 2353–2362.

7. Chen, M., Ju, M.-G., Carl, A.D., Zong, Y., Grimm, R.L., Gu, J., Zeng, X.C., Zhou, Y., and Padture, N.P. (2018). Cesium titanium(IV) bromide thin films based stable lead-free perovskite solar cells. Joule *2*, 558–570.

8. Correa-Baena, J.-P., Nienhaus, L., Kurchin, R.C., Shin, S.S., Wieghold, S., Putri Hartono, N.T., Layurova, M., Klein, N.D., Poindexter, J.R., Polizzotti, A., et al. (2018). A-site cation in inorganic $A_3Sb_2I_9$ perovskite influences structural dimensionality, exciton binding energy, and solar cell performance. Chem. Mater. *30*, 3734–3742.

9. Abate, A. (2017). Perovskite solar cells go lead free. Joule *1*, 659–664.

10. Garrett, J.L., Tennyson, E.M., Hu, M., Huang, J., Munday, J.N., and Leite, M.S. (2017). Real-time nanoscale open-circuit voltage dynamics of perovskite solar cells. Nano Lett. *17*, 2554–2560.

11. Howard, J.M., Tennyson, E.M., Barik, S., Szostak, R., Waks, E., Toney, M.F., Nogueira, A.F., Neves, B.R.A., and Leite, M.S. (2018). Humidity-induced photoluminescence hysteresis in variable Cs/Br ratio hybrid perovskites. J. Phys. Chem. Lett. *9*, 3463–3469.

12. Domanski, K., Alharbi, E.A., Hagfeldt, A., Gratzel, M., and Tress, W. (2018). Systematic investigation of the impact of operation conditions on the degradation behaviour of perovskite solar cells. Nat. Energy *3*, 61–67.

13. Domanski, K., Roose, B., Matsui, T., Saliba, M., Turren-Cruz, S.H., Correa-Baena, J.P., Carmona, C.R., Richardson, G., Foster, J.M., De Angelis, F., et al. (2017). Migration of cations induces reversible performance losses over day/night cycling in perovskite solar cells. Energy Environ. Sci. *10*, 604–613.

14. Takahashi, K., Takahashi, L., Miyazato, I., and Tanaka, Y. (2018). Searching for hidden perovskite materials for photovoltaic systems by combining data science and first principle calculations. ACS Photon. *5*, 771–775.

15. Berhe, T.A., Su, W.-N., Chen, C.-H., Pan, C.-J., Cheng, J.-H., Chen, H.-M., Tsai, M.-C., Chen, L.-Y., Dubale, A.A., and Hwang, B.-J. (2016). Organometal halide perovskite solar cells: degradation and stability. Energy Environ. Sci. *9*, 323–356.

16. Deretzis, I., Smecca, E., Mannino, G., La Magna, A., Miyasaka, T., and Alberti, A. (2018). Stability and degradation in hybrid perovskites: is the glass half-empty or half-full? J. Phys. Chem. Lett. *9*, 3000–3007.

17. Hu, J.G., Gottesman, R., Gouda, L., Kama, A., Priel, M., Tirosh, S., Bisquert, J., and Zaban, A. (2017). Photovoltage behavior in perovskite solar cells under light-soaking showing photoinduced interfacial changes. ACS Energy Lett. *2*, 950–956.

18. Khenkin, M.V., Annop, K.M., Visoly-Fisher, I., Kolusheva, S., Galagan, Y., Di Giacomo, F., Vukovic, O., Patil, B.R., Sherafatipour, G., Turkovic, V., et al. (2018). Dynamics of photoinduced degradation of perovskite photovoltaics: from reversible to irreversible processes. ACS Appl. Energy Mater. *1*, 799–806.

19. Huang, F., Jiang, L., Pascoe, A.R., Yan, Y., Bach, U., Spiccia, L., and Cheng, Y.-B. (2016). Fatigue behavior of planar $CH_3NH_3PbI_3$ perovskite solar cells revealed by light on/off diurnal cycling. Nano Energy *27*, 509–514.

20. Khenkin, M.V., Anoop, K.M., Visoly-Fisher, I., Galagan, Y., Di Giacomo, F., Patil, B.R., Sherafatipour, G., Turkovic, V., Rubahn, H.G., Madsen, M., et al. (2018). Reconsidering figures of merit for performance and stability of perovskite photovoltaics. Energy Environ. Sci. *11*, 739–743.

21. Aristidou, N., Eames, C., Sanchez-Molina, I., Bu, X., Kosco, J., Islam, M.S., and Haque, S.A. (2017). Fast oxygen diffusion and iodide defects mediate oxygen-induced degradation of perovskite solar cells. Nat. Commun. *8*, 15218.

22. Bryant, D., Aristidou, N., Pont, S., Sanchez-Molina, I., Chotchunangatchaval, T., Wheeler, S., Durrant, J.R., and Haque, S.A. (2016). Light and oxygen induced degradation limits the operational stability of methylammonium lead triiodide perovskite solar cells. Energy Environ. Sci. *9*, 1655–1660.

23. Huang, W., Manser, J.S., Kamat, P.V., and Ptasinska, S. (2016). Evolution of chemical composition, morphology, and photovoltaic efficiency of $CH_3NH_3PbI_3$ perovskite under ambient conditions. Chem. Mater. *28*, 303–311.

24. Christians, J.A., Miranda Herrera, P.A., and Kamat, P.V. (2015). Transformation of the excited state and photovoltaic efficiency of $CH_3NH_3PbI_3$ perovskite upon controlled exposure to humidified air. J. Am. Chem. Soc. *137*, 1530–1538.

25. Leguy, A.M.A., Hu, Y., Campoy-Quiles, M., Alonso, M.I., Weber, O.J., Azarhoosh, P., van Schilfgaarde, M., Weller, M.T., Bein, T., Nelson, J., et al. (2015). Reversible hydration of $CH_3NH_3PbI_3$ in films, single crystals, and solar cells. Chem. Mater. *27*, 3397–3407.

26. Hall, G.N., Stuckelberger, M., Nietzold, T., Hartman, J., Park, J.-S., Werner, J., Niesen, B., Cummings, M.L., Rose, V., Ballif, C., et al. (2017). The role of water in the reversible optoelectronic degradation of hybrid perovskites at low pressure. J. Phys. Chem. C *121*, 25659–25665.

27. Snaith, H.J., Abate, A., Ball, J.M., Eperon, G.E., Leijtens, T., Noel, N.K., Stranks, S.D., Wang, J.T., Wojciechowski, K., and Zhang, W. (2014). Anomalous hysteresis in perovskite solar cells. J. Phys. Chem. Lett. *5*, 1511–1515.

28. Divitini, G., Cacovich, S., Matteocci, F., Cina, L., Di Carlo, A., and Ducati, C. (2016). In situ observation of heat-induced degradation of perovskite solar cells. Nat. Energy *1*, 15012.

29. Hoke, E.T., Slotcavage, D.J., Dohner, E.R., Bowring, A.R., Karunadasa, H.I., and McGehee, M.D. (2015). Reversible photo-induced trap formation in mixed-halide hybrid perovskites for photovoltaics. Chem. Sci. *6*, 613–617.

30. Braly, I.L., Stoddard, R.J., Rajagopal, A., Uhl, A.R., Katahara, J.K., Jen, A.K.Y., and Hillhouse, H.W. (2017). Current-induced phase segregation in mixed halide hybrid perovskites and its impact on two-terminal tandem solar cell design. ACS Energy Lett. *2*, 1841–1847.

31. Quitsch, W.A., deQuilettes, D.W., Pfingsten, O., Schmitz, A., Ognjanovic, S., Jariwala, S., Koch, S., Winterer, M., Ginger, D.S., and Bacher, G. (2018). The role of excitation energy in photobrightening and photodegradation of halide perovskite thin films. J. Phys. Chem. Lett. *9*, 2062–2069.

32. Motti, S.G., Gandini, M., Barker, A.J., Ball, J.M., Kandada, A.R.S., and Petrozza, A. (2016). Photoinduced emissive trap states in lead halide perovskite semiconductors. ACS Energy Lett. *1*, 726–730.

33. Lee, S.W., Kim, S., Bae, S., Cho, K., Chung, T., Mundt, L.E., Lee, S., Park, S., Park, H., Schubert, M.C., et al. (2016). UV degradation and recovery of perovskite solar cells. Sci. Rep. *6*, 38150.

34. Tennyson, E.M., Gong, C., and Leite, M.S. (2017). Imaging energy harvesting and storage systems at the nanoscale. ACS Energy Lett. *2*, 2761–2777.

35. Tennyson, E.M., Garrett, J.L., Frantz, J.A., Myers, J.D., Bekele, R.Y., Sanghera, J.S., Munday, J.N., and Leite, M.S. (2015). Nanoimaging of open-circuit voltage in photovoltaic devices. Adv. Energy Mater. *5*, 1501142.

36. Tennyson, E.M., Howard, J.M., and Leite, M.S. (2017). Mesoscale functional imaging of materials for photovoltaics. ACS Energy Lett. *2*, 1825–1834.

37. Leite, M.S., Abashin, M., Lezec, H.J., Gianfrancesco, A., Talin, A.A., and Zhitenev, N.B. (2014). Nanoscale imaging of photocurrent and efficiency in CdTe solar cells. ACS Nano *8*, 11883–11890.

38. Garrett, J.L., Leite, M.S., and Munday, J.N. (2018). Multiscale functional imaging of interfaces through atomic force microscopy using harmonic mixing. ACS Appl. Mater. Interfaces *10*, 28850–28859.

39. Tian, Y., Peter, M., Unger, E., Abdellah, M., Zheng, K., Pullerits, T., Yartsev, A., Sundstrom, V., and Scheblykin, I.G. (2015). Mechanistic insights into perovskite photoluminescence enhancement: light curing with oxygen can boost yield thousandfold. Phys. Chem. Chem. Phys. *17*, 24978–24987.

40. Li, C., Guerrero, A., Zhong, Y., Graser, A., Luna, C.A.M., Kohler, J., Bisquert, J., Hildner, R., and Huettner, S. (2017). Real-time observation of iodide ion migration in methylammonium lead halide perovskites. Small *13*, 1701711.

41. Kutes, Y., Zhou, Y., Bosse, J.L., Steffes, J., Padture, N.P., and Huey, B.D. (2016). Mapping the photoresponse of $CH_3NH_3PbI_3$ hybrid perovskite thin films at the nanoscale. Nano Lett. *16*, 3434–3441.

42. Conings, B., Drijkoningen, J., Gauquelin, N., Babayigit, A., D'Haen, J., D'Olieslaeger, L., Ethirajan, A., Verbeeck, J., Manca, J., Mosconi, E., et al. (2015). Intrinsic thermal instability of methylammonium lead trihalide perovskite. Adv. Energy Mater. *5*, 1500477.

43. deQuilettes, D.W., Zhang, W., Burlakov, V.M., Graham, D.J., Leijtens, T., Osherov, A., Bulovic, V., Snaith, H.J., Ginger, D.S., and Stranks, S.D. (2016). Photo-induced halide redistribution in organic-inorganic perovskite films. Nat. Commun. *7*, 11683.

44. El-Hajje, G., Momblona, C., Gil-Escrig, L., Avila, J., Guillemot, T., Guillemoles, J.F., Sessolo, M., Bolink, H.J., and Lombez, L. (2016). Quantification of spatial inhomogeneity in perovskite solar cells by hyperspectral luminescence imaging. Energy Environ. Sci. *9*, 2286–2294.

45. Collins, L., Ahmadi, M., Qin, J., Liu, Y., Ovchinnikova, O.S., Hu, B., Jesse, S., and Kalinin, S.V. (2018). Time resolved surface photovoltage measurements using a big data capture approach to KPFM. Nanotechnology *29*, 445703.

46. Haber, J.A., Cai, Y., Jung, S., Xiang, C., Mitrovic, S., Jin, J., Bell, A.T., and Gregoire, J.M. (2014). Discovering Ce-rich oxygen evolution catalysts, from high throughput screening to water electrolysis. Energy Environ. Sci. *7*, 682–688.

47. Game, O.S., Buchsbaum, G.J., Zhou, Y., Padture, N.P., and Kingon, A.I. (2017). Ions matter: description of the anomalous electronic behavior in methylammonium lead halide perovskite devices. Adv. Funct. Mater. *27*, 1606584.

48. Banse, D., Doddington, G.R., Garcia-Romero, D., Godfrey, J.J., Greenberg, C.S., Hernandez-Cordero, J., Howard, J.M., Martin, A.F., Mason, L.P., McCree, A., et al. (2015). Analysis of the second phase of the 2013-2014 i-Vector machine learning challenge. 16th Annual Conference of the International Speech Communication Association (Interspeech 2015), Vols. 1–5, 3041–3045.

49. Martin, A.F., Greenberg, C.S., Stanford, V.M., Howard, J.M., Doddington, G.R., and Godfrey, J.J. (2014). Performance factor analysis for the 2012 NIST speaker recognition evaluation. 15th Annual Conference of the International Speech Communication Association (Interspeech 2014), Vols. 1–4, 1135–1138.

50. Laptev, N., Yosinski, J., Li, L.E., and Smyl, S. (2017). Time-series extreme event forecasting with neural networks at Uber. Paper presented at: International Conference on Machine Learning.

51. Ma, X., Tao, Z., Wang, Y., Yu, H., and Wang, Y. (2015). Long short-term memory neural network for traffic speed prediction using remote microwave sensor data. Transport. Res. C Emerg. Tech. *54*, 187–197.

52. Jordan, M.I., and Mitchell, T.M. (2015). Machine learning: trends, perspectives, and prospects. Science *349*, 255–260.

53. Jo, T., Hou, J., Eickholt, J., and Cheng, J. (2015). Improving protein fold recognition by deep learning networks. Sci. Rep. *5*, 17573.

54. Jaeger, H., and Haas, H. (2004). Harnessing nonlinearity: predicting chaotic systems and saving energy in wireless communication. Science *304*, 78–80.

55. Sun, Y.C., Szucs, G., and Brandt, A.R. (2018). Solar PV output prediction from video streams using convolutional neural networks. Energy Environ. Sci. *11*, 1811–1818.

56. Abadi, M., Barham, P., Chen, J., Chen, Z., Davis, A., Dean, J., Devin, M., Ghemawat, S., Irving, G., and Isard, M. (2016). TensorFlow: a system for large-scale machine learning. Paper presented at: 12th USENIX Symposium on Operating Systems Design and Implementation.

57. Suram, S.K., Xue, Y., Bai, J., Le Bras, R., Rappazzo, B., Bernstein, R., Bjorck, J., Zhou, L., van Dover, R.B., Gomes, C.P., et al. (2017). Automated phase mapping with AgileFD and its application to light absorber discovery in the V-Mn-Nb oxide system. ACS Comb. Sci. *19*, 37–46.

58. Correa-Baena, J.P., Hippalgaonkar, K., van Duren, J., Jaffer, S., Chandrasekhar, V.R., Stevanovic, V., Wadia, C., Guha, S., and Buonassisi, T. (2018). Accelerating materials development via automation, machine learning, and high-performance computing. Joule *2*, 1410–1420.

59. Schmidt, J., Shi, J., Borlido, P., Chen, L., Botti, S., and Marques, M.A.L. (2017). Predicting the thermodynamic stability of solids combining density functional theory and machine learning. Chem. Mater. *29*, 5090–5103.

60. Pilania, G., Mannodi-Kanakkithodi, A., Uberuaga, B.P., Ramprasad, R., Gubernatis, J.E., and Lookman, T. (2016). Machine learning bandgaps of double perovskites. Sci. Rep. *6*, 19375.

61. Chakraborty, S., Xie, W., Mathews, N., Sherburne, M., Ahuja, R., Asta, M., and Mhaisalkar, S.G. (2017). Rational design: a high-throughput computational screening and experimental validation methodology for lead-free and emergent hybrid perovskites. ACS Energy Lett. *2*, 837–845.

62. Schalkoff, R.J. (1997). Artificial Neural Networks (McGraw-Hill).

63. Titano, J.J., Badgeley, M., Schefflein, J., Pain, M., Su, A., Cai, M., Swinburne, N., Zech, J., Kim, J., Bederson, J., et al. (2018). Automated deep-neural-network surveillance of cranial images for acute neurologic events. Nat. Med. *24*, 1337–1341.

64. Hochreiter, S., and Schmidhuber, J. (1997). Long short-term memory. Neural Comput. *9*, 1735–1780.

65. Chen, K., Zhou, Y., and Dai, F.Y. (2015). A LSTM-based method for stock returns prediction: a case study of China stock market. Proceedings 2015 IEEE International Conference on Big Data, 2823–2824.

66. Mangan, N.M., Kutz, J.N., Brunton, S.L., and Proctor, J.L. (2017). Model selection for dynamical systems via sparse regression and information criteria. Proc. Royal Soc. A *473*, 20170009.

67. Saliba, M., Stolterfoht, M., Wolff, C.M., Neher, D., and Abate, A. (2018). Measuring aging stability of perovskite solar cells. Joule *2*, 1019–1024.

68. Silverman, T.J., Deceglie, M.G., Sun, X., Garris, R.L., Alam, M.A., Deline, C., and Kurtz, S. (2015). Thermal and electrical effects of partial shade in monolithic thin-film photovoltaic modules. IEEE J. Photovolt. *5*, 1742–1747.

69. Bowring, A.R., Bertoluzzi, L., O'Regan, B.C., and McGehee, M.D. (2018). Reverse bias behavior of halide perovskite solar cells. Adv. Energy Mater. *8*, 1702365.

70. Raccuglia, P., Elbert, K.C., Adler, P.D.F., Falk, C., Wenny, M.B., Mollo, A., Zeller, M., Friedler, S.A., Schrier, J., and Norquist, A.J. (2016). Machine-learning-assisted materials discovery using failed experiments. Nature *533*, 73.